PEER-REVIEWED ARTICLE

Relative Radiometric Normalization of Landsat Multispectral Scanner (MSS) Data Using an Automatic Scattergram-Controlled Regression

Christopher D. Elvidge, Ding Yuan, Ridgeway D. Weerackoon, and Ross S. Lunetta

Abstract

A relative radiometric normalization (RRN) based on an Automatic Scattergram-Controlled Regression (ASCR) has been developed to create radiometrically comparable multispectral data sets, compensating for radiometric divergence present in images acquired under different illumination, atmospheric, or sensor conditions. The ASCR procedure locates the statistical centers for stable land and stable water data clusters using the near-infrared date 1 versus date 2 scattergrams to establish an initial regression line. Thresholds are placed about the initial line to select a "no-change" pixel set, which is used in the regression analysis of each band to derive gains and off sets for the radiometric normalization. The ASCR procedure was designed for preparing large numbers of multitemporal Landsat data sets for digital detection of land-cover change.

Introduction

The scientific requirement for increased understanding of human impacts on terrestrial carbon stocks and biodiversity has created renewed interest in the use of Landsat Multispectral Scanner (MSS) data for the analysis of land-cover change (Lunetta *et al.*, 1993). A series of five Landsat MSS sensors were used to acquire Earth observations over a 21-year period (1972-1992), forming the longest available set of repetitive satellite observations of the Earth's surface.

Land-cover changes generally alter the reflectance of the land surface, which can be detected using multitemporal Landsat data sets. The analysis of land-cover change using multitemporal Landsat data is complicated by the presence of substantial radiometric differences between Landsat scenes (Markham and Barker, 1987). Because Landsat MSS had no on-board calibration system, there are uncorrected radiometric differences between data acquired by different sensors (e.g., Landsat 1 versus Landsat 5). There was also drift in the radiometric performance of the individual sensors over time. In addition, there were changes in the ground processing procedures between 1972 and 1992 which resulted in radiometric differences between scenes present in the archives. Variations in solar illumination conditions, atmospheric scattering, and atmospheric absorption result in differences in the at-sensor radiance values that are unrelated to the reflectance of the land surface.

Given sufficient time and resources, it would be possible to model or calibrate each of these effects and generate multispectral datasets in physical measurement units (e.g., ground radiance or ground reflectance) for use in the analysis of land-cover change. However, for large scale projects where change detection products are to be generated for the hundreds of scenes required to cover a continental size area, it would be advantageous to use an automated approach to perform a relative radiometric normalization of scenes in a single set of steps.

Relative radiometric normalizations use one image as a reference and adjust the radiometric properties of subject image(s) to match the reference (Hall *et al.*, 1991). One advantage of these procedures is that the original radiometric condition of the reference image is retained, obviating the computational effort required to convert each image to units of radiance or reflectance. In this paper we describe an Automatic Scattergram-Controlled Regression (ASCR) method that we have developed for performing relative radiometric normalization on large numbers of Landsat data sets.

Background

Relative radiometric normalization techniques are based on the linear comparison of the statistical characteristics of two images or of selected spectral control subsets from two images. These empirical methods have a similar linear transformation form $\hat{x}_k = a_k x_k + b_k$, where x_k is the kth band of the subject image X, $\hat{x}_k$ is the kth band of resulting normalized image, and a_k and b_k are the gain and offset used to achieve normalization of band k in image X.

Regression-based approaches to relative radiometric normalization have been recognized for many years (Jenson,

C.D. Elvidge is with the Desert Research Institute and Nevada Agricultural Experiment Station, Reno, NV 89506.

D Yuan and R.D. Weerackoon are with the Biological Sciences Center, Desert Research Institute, Las Vegas, NV 89132.

R.S. Lunetta is with the Environmental Monitoring Systems Laboratory, U.S. Environmental Protection Agency, Las Vegas, NV 89119.

Photogrammetric Engineering & Remote Sensing, Vol. 61, No. 10, October 1995, pp. 1255–1260.

0099-1112/95/6110-1255$3.00/0
© 1995 American Society for Photogrammetry and Remote Sensing

1983). Regression techniques are based on the observation that within a given spectral band there is an overall linear relationship between the digital number (DN) values for two images acquired of the same ground area. In image pairs where such linearity exists, regression analysis can be used to derive a gain and offset for radiometrically normalizing the subject image to match the reference image. In the Simple Regression (SR) normalization, the full contents of scenes are analyzed using a linear regression (Jenson, 1983). Successful application of the SR normalization requires image pairs that are devoid of statistical ouliers which are present in only one of the images (e.g., clouds). In addition, the SR normalization should only be applied to images in which the vegetation is at a comparable growth stage (phenology).

The SR method works well where there are no major clouds or other phenomena present at one date but absent at the other. Other procedures have been developed to select subsets of the image contents, believed to be spectrally stable, for use in radiometric normalization procedures. Schott *et al.* (1988) developed a Pseudo-Invariant Feature (PIF) method which applies a threshold to the ratio of the near-infrared/red spectral bands to locate a set of land surface pixels in each image with low green vegetation cover. In the PIF method, the gains and offsets that are applied to the subject image are determined based on the linear shift required to make the mean and standard deviation of the subject pixel set match the reference image pixel set. Hall *et al.* (1991) devised an approach which uses dark and bright pixel sets selected independently from each image based on a greenness-brightness transformation (Kauth and Thomas, 1976). The dark set typically consists of deep water pixels and the bright set contains land surface pixels containing bright materials (e.g., soils or concrete) and little green vegetation. The mean values for the dark and bright pixel sets in each image are used to define a gain and offset for each spectral band, which is then applied to the full subject scene. It should be noted that, in both of these procedures (Schott *et al.*, 1988; Hall *et al.*, 1991), the subject and reference pixel sets are not required to be colocated within the scene.

Yuan and Elvidge (1993) developed a Scattergram-Controlled Regression (SCR) for use in the digital detection of land-cover change using Landsat MSS data. Instead of using the whole image to derive gains and offsets as in the SR method, the SCR approach uses pixels from a region of "no change" identified using scattergrams. By identifying a "no-change" pixel set, it is possible to avoid the use of pixels containing cloud, cloud-shadow, and land-cover change in the regression analysis. The SCR procedure assumes that the majority of pixels in a scene have the same land cover and phenological (vegetation growth) stage for both image dates. The "no-change" pixels were manually selected based on scattergrams of the near-infrared data from the subject versus the reference images. The near-infrared data were used because at these wavelengths the spectral clusters for water and land are clearly separated, and a distinct axis of "no change" can be observed. An analyst examines the scattergram and selects and initial line of "no change." An envelope of ten DNs above and below the initial line defined the "no-change" pixels, and these pixels were then used to perform the regression to derive the normalization gain and offset for each spectral band. The disadvantage of the SCR method is that it requires a visual determination of the initial position of the axis of no change.

In this paper we present improvements made to the SCR method in order to increase automation of the procedure. The following text describes our current method for an Automated Scattergram-Controlled Regression (ASCR).

Study Area

We selected Landsat MSS scenes from the Washington, D.C., area for 25 June 1990 (Plate 1a) and 8 July 1973 (Plate 1b) for our research. The data sets were preprocessed by the U.S. Geological Survey EROS Data Center for the U.S. EPA North American Landscape Characterization (NALC) project. The NALC preprocessing included geometric registration and resampling the data to a common 60-metre grid in a Universal Transverse Mercator projection (Lunetta *et al.*, 1993).

Our initial examination of the two scenes indicated that they are very different from each other radiometrically even though the images were processed identically. The 1990 data were contrast stretched, then the 1990 contrast stretch was applied to the 1973 image. Relative to the 1990 image, the 1973 image has a duller appearance, with less contrast than the 1990 image. The 1973 image has a bluish tinge to it, as if there were more haze present. It is not possible to say from this observation alone that the 1973 data had more haze or not, because we are dealing with uncalibrated data. One area of light cirrus cloud cover can be observed slightly to the left of the 1973 image center. The 1990 image contains substantial cloud cover and associated shadow.

Scattergrams

The description of the ASCR procedures will be with reference to the scattergrams presented in Figure 1 and the histograms presented in Figure 2. Figure 1 shows the 1990 versus 1973 full-scene scattergrams for each spectral band. Large numbers of pixels fall onto the same locations in the densest regions of the scattergrams; therefore, an exponential stretch was applied to visually enhance the relative magnitude of pixel concentrations for elements of the scattergram matrix. The regions having the densest numbers of pixels are shown in white, surrounded by zones of gray and black, indicating declining numbers of pixels. Areas outside the data cluster, having no pixels present, are white.

Figure 1a shows the scattergram for Band 1 (0.5 to 0.6 μm) data from 1973 and 1990. The scattergram shows a single dense data cluster containing land and water pixels. The 1990 cloud and cloud-contaminated pixels have anomalously higher 1990 DN values and are pulled away from the land-water data cluster along the 1990 data axis. There are a large number of 1990 cloud pixels with saturated DN values in Band 1 (DN = 127). The fact that the 1973 image had more haze or atmospheric scattering present than the 1990 image is illustrated by the larger offset from the origin to the dense land-water data cluster along the 1973 DN axis relative to the 1990 DN axis. This relationship is repeated to a lesser degree in Bands 2 and 3.

Figure 1b shows Band 2 (0.6 to 0.7 μm) data for 1973 versus 1990. The Band 2 and Band 1 scattergrams show the same basic features. The lower end of the dense data cloud for Band 2 is closer to the origin than in Band 1 because there is less atmospheric scattering in Band 2 than in Band 1.

Figure 1c for Band 3 (0.7 to 0.8 μm) and Figure 1d for Band 4 (0.8 to 1.1 μm) show similar features. In the near-infrared, water is much darker than the land surface, resulting in two dense data clusters: a compact data cluster for water near the origin, and an elliptical data cluster for land-surface pixels near the center of the scattergram. Clusters of 1990

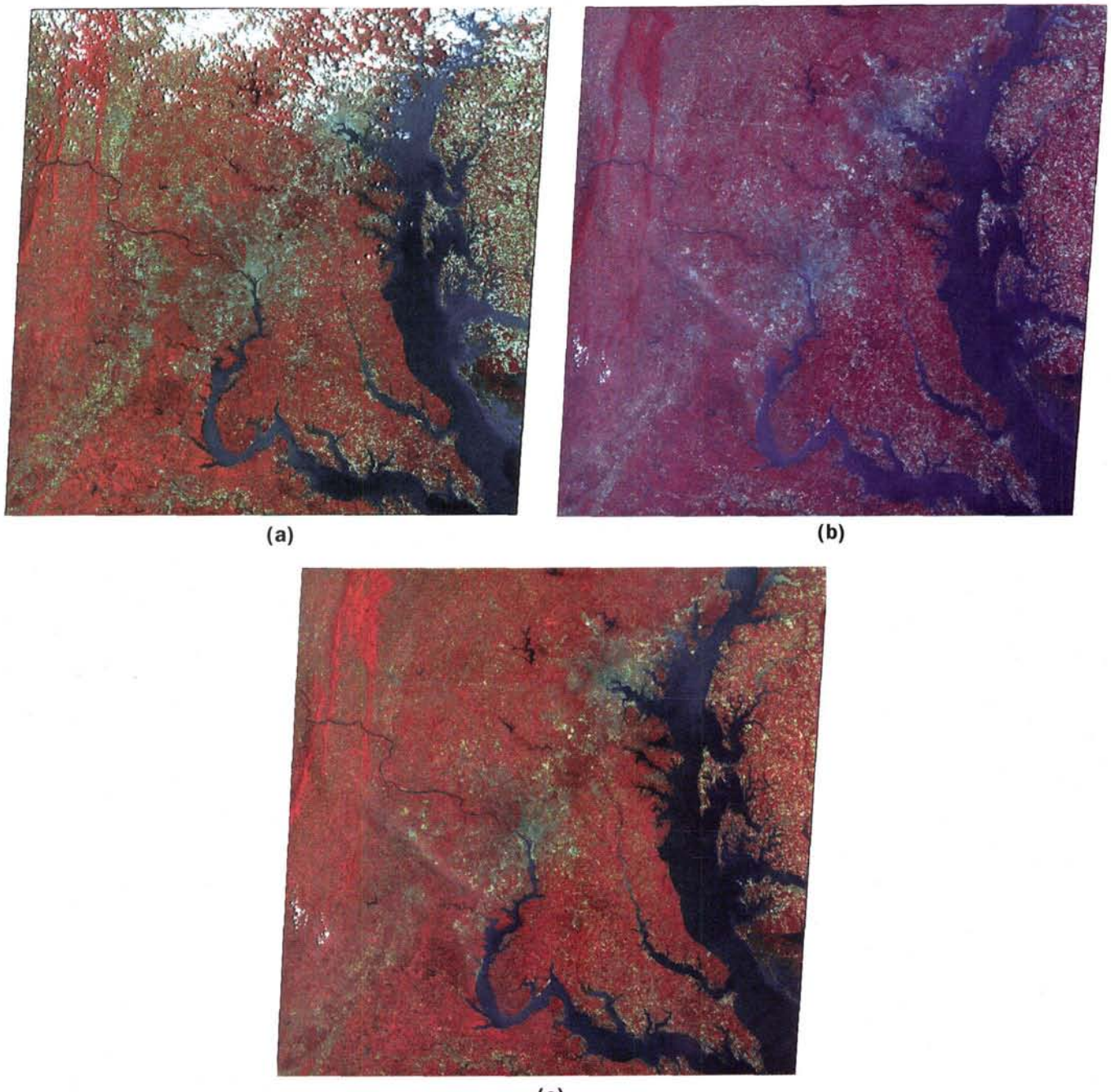

(a) (b) (c)

Plate 1. False color images of Landsat MSS Path 15 Row 33 of the Washington, D.C., area. The images were formed using bands 1, 2, and 4 as blue, green, and red. The same contrast stretch was applied to each image. (a) 25 June 1990 image with linear contrast stretch. (b) 8 July 1973 image with the same contrast stretch as (a). (c) ASCR normalized 8 July 1973 image with the same contrast stretch as (a).

cloud and cloud-contaminated pixels rise along the 1990 axis from both the water- and land-surface dense data clusters. In addition, there are data lobes protruding below the land data clusters, resulting from shadow and shadow-contaminated pixels present in the 1990 dataset.

Methods

The ASCR procedure involves the identification of a "no-change" pixel set, taken to be those pixels occupying the core of the water and land data clusters observable in the near-infrared (Bands 3 and 4) scattergrams. Regression is

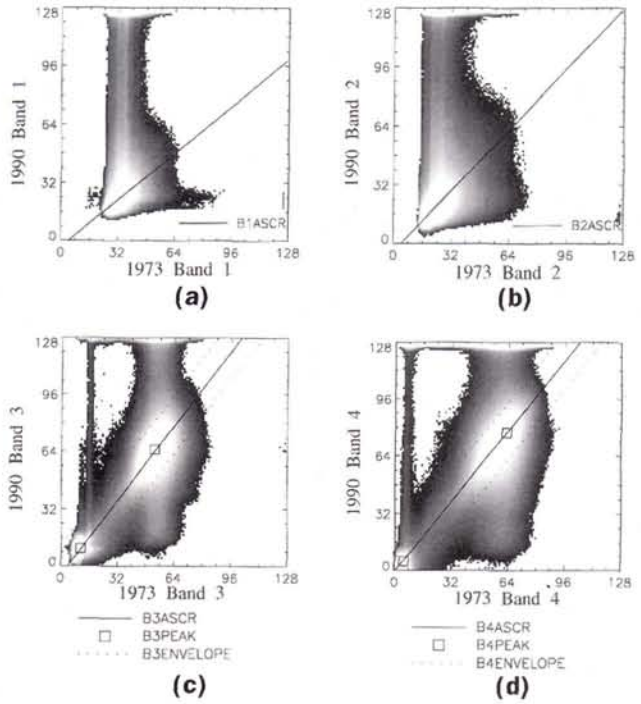

Figure 1. Band-by-band full scene scattergrams for the 1990 versus 1973 Landsat MSS data. (a) Scattergram of the 1990 Band 1 versus 1973 Band 1. (b) Scattergram of the 1990 Band 2 versus 1973 Band 2. (c) Scattergram of 1990 Band 3 versus 1973 Band 3. (d) Scattergram of 1990 Band 4 versus 1973 Band 4.

then used to derive the gains and offsets used to radiometrically normalize the subject image (X) to match the reference image (Y).

Four procedures are used in ASCR normalization:

Procedure 1: Compute scattergrams of image X and Y for the near-infrared bands (Figures 1c and 1d). For Landsat MSS, the image X versus image Y scattergram for a band is a 127 by 127 matrix. The matrix is filled with the numbers of pixels having the indicated image X versus image Y digital number (DN) values. We refer to the Band 3 scattergram as F_3 and the Band 4 scattergram as F_4.

Procedure 2: A search is conducted to locate the centers of the water- and land-surface data clusters based on the local maxima for the near-infrared band scattergrams (i.e., the scattergram cells having the maximum number of water and land pixels). The water data-cluster center is located at low DN values near the lower left corner of the scattergrams, not far from the origin. The center of the land-surface data cluster is located near the center of the scattergram. To locate the land and water data-cluster center points, we search $F_{3lmax} = F_3(i_{lmax3}, j_{lmax3})$, $F_{3umax} = F_3(i_{umax3}, j_{umax3})$, $F_{4lmax} = F_4(i_{lmax4}, j_{lmax4})$, and $F_{4umax} = F_4(i_{umax4}, j_{umax4})$, where i = row locations in the scattergram; j = column locations in the scattergram; F_{3lmax}, F_{3umax}, F_{4lmax}, and F_{4umax} are the corresponding lower (water) maxima and upper (land) maxima of F_3 and F_4; (i_{lmax3}, j_{lmax3}) and (i_{umax3}, j_{umax3}) are the corresponding vertical and horizontal locations of the maxima for Band 3; and (i_{lmax4}, j_{lmax4}) and (i_{umax4}, j_{umax4}) are the corresponding vertical and horizontal locations of the maxima for Band 4. These locations are taken as the centers for the land and water data clusters.

This procedure is presented graphically in Figure 2 using a histogram indicating the maximum number of image Y pixels occupying a single matrix cell for a given image X DN value. For each band, three local maxima can be observed: (1) at the low 1990 DN values there is a local maxima for those pixels which were water on both dates; (2) at the middle of the histogram there is a second local maxima, representing the center of the land-surface data cluster on the scattergram; and (3) a third local maxima, representing 1990 cloud pixels, is located at the high 1990 DN end of the histogram. Many of these cloud pixels have saturated DN counts of 127. The 1973 DN values for the scattergram cells selected for the histogram are indicated with "+" marks. The scattergram cells producing the local maxima for water and land are indicated with labels.

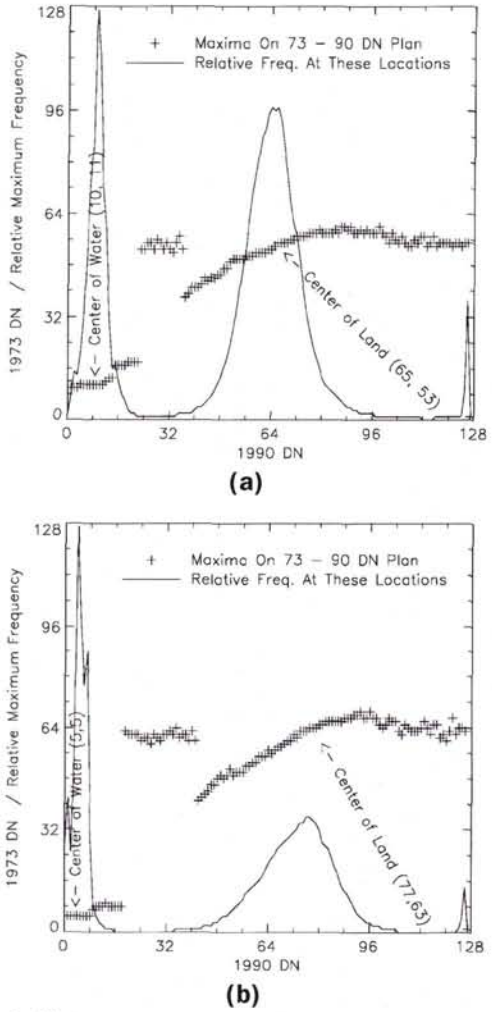

Figure 2. Histograms used to select the local maxima of the Band 3 and 4 scattergrams. (a) Local maxima distribution for Band 3. (b) Local maxima distribution for Band 4.

TABLE 1. THE NO-CHANGE REGION IN THE EXPERIMENT WAS DETERMINED BY THE INTERSECT OF BAND 3 AND BAND 4 NO-CHANGE REGIONS. THE NO-CHANGE REGION FOR A PARTICULAR BAND IS DETERMINED BY LINKING THE CENTER OF WATER AND CENTER OF LAND FOR THAT BAND AND EXPANDING PERPENDICULARLY TO THE WATER-LAND LINE UP TO TEN DIGITAL NUMBERS (HPW) ON EITHER SIDE OF THE LINE.

Positions (1990, 1973)	Center of Water	Center of Land	HPW	HVW
Band 3	(10,11)	(65,53)	10	16.48
Band 4	(5,5)	(77,63)	10	15.94

Once the above centers are determined, coefficients (a = gain, b = offset) are computed for an initial "no-change" axes for Band 3 and Band 4 from the positions of the land and water data-cluster centers. That is, let

$$a_{3_0} = \frac{j_{umax3} - j_{lmax3}}{i_{umax3} - i_{lmax3}}$$

$$b_{3_0} = j_{lmax3} - a_{3_0} * i_{lmax3}$$

$$a_{4_0} = \frac{j_{umax4} - j_{lmax4}}{i_{umax4} - i_{lmax4}}$$

$$b_{4_0} = j_{lmax4} - a_{4_0} * i_{lmax4}$$

The no-change region is defined based on HPW_{NC}, the estimated half perpendicular width of the no-change region for the Band 3 and Band 4 scattergrams (Figure 1). In computation, only the half vertical width HVW_{NC} of the no-change region is used. HPW_{NC} and HVW_{NC} have the following relationship:

$$HVW_{NC} = \sqrt{1 + a_0^2}\,(HPW_{NC})$$

where a_0 is the slope of the initially estimated axis for a given band. For our initial effort, an HPW_{NC} value of 10 digital numbers has been used. We are currently experimenting with an automated selection of HVW_{NC} based on the width of the land and water data clusters on Figure 2 at a fixed percentage (e.g., 50 percent) of the peak height.

The NC (*no-change*) pixel set is then selected as

$$NC = (x,y) : |y_3 - b_{3_0} - a_{3_0} x_3| \le HVW_{NC_3} \text{ and}$$
$$|y_4 - b_{4_0} - a_{4_0} x_4| \le HVW_{NC_4}$$

Procedure 3: Compute regression lines for all four bands. Only pixels falling into region NC, determined based on the Band 3 and Band 4 scattergrams, are used for regression (Figure 1). The regression coefficients for band k are computed from a least-squares equation: i.e.,

TABLE 2. THE STATISTICS OF THE NO-CHANGE REGION FOR THE EXPERIMENTAL IMAGES.

	Subject Image (1973)		Reference Image (1990)		
Band	Mean	Variance	Mean	Variance	Covariance
1	33.32	23.02	23.72	44.26	18.34
2	23.29	43.70	20.10	105.34	41.94
3	45.61	295.42	54.14	531.42	382.58
4	48.98	516.87	59.22	808.60	628.14

TABLE 3. COMPARISON OF THE INITIAL ESTIMATIONS AND FINAL ESTIMATIONS FOR THE NORMALIZATION LINES FOR THE EXPERIMENTAL IMAGE DATA. THE RMSS ARE THE ROOT MEAN SQUARES FOR THE NO-CHANGE REGION FOR CORRESPONDING NORMALIZATION LINES.

	Initial estimates from scattergrams			Refined estimates through regression		
Band	a_{k_0}	b_{k_0}	RMS_k	a_k	b_k	RMS_k
1				0.7965	−2.8161	5.4460
2				0.9597	−2.2535	6.0677
3	1.3095	−4.4048	6.1174	1.2951	−4.9246	5.9973
4	1.2414	−1.2069	6.7622	1.2153	−0.3041	6.7257

$$Q_k = \sum_{NC} (y_k - b_k - a_k x_k)^2 = \min$$

where NC is the number of "no-change" pixels.

To solve this equation, one obtains the rectification coefficients

$$a_k = s^{(nc)}_{x_k y_k} / s^{(nc)}_{x_k x_k} \quad (1)$$

$$b_k = \bar{y}_k^{(nc)} - a_k \bar{x}_k^{(nc)} \quad (2)$$

where $\bar{x}_k^{(nc)}$ and $\bar{y}_k^{(nc)}$ are the means of the no-change region on two dates, $s^{(nc)}_{x_k x_k}$ is the sample variance of x_k, and $s^{(nc)}_{x_k y_k}$ is the sample covariance of x_k, and y_k in the no-change region. That is,

$$\bar{x}_k^{(nc)} = \frac{1}{|NC|} \sum_{NC} x_k$$

$$\bar{Y}_k^{(nc)} = \frac{1}{|NC|} \sum_{NC} y_k$$

$$s^{(nc)}_{x_k x_k} = \frac{1}{|NC|} \sum_{NC} (x_k - \bar{x}_k^{(nc)})^2$$

$$s^{(nc)}_{x_k y_k} = \frac{1}{|NC|} \sum_{NC} (x_k - \bar{x}_k^{(nc)})\,(y_k - \bar{y}_k^{(nc)})$$

Procedure 4: Normalize image X using coefficients computed above. That is, for $k = 1, 2, 3, 4$, compute

$$\hat{x}_k = a_k x_k + b_k$$

Results

The location for the center of water is (10,11) for Band 3 and (5,5) for Band 4. The location for the center of land surface is (65,53) for Band 3 and (77,63) for Band 4 (Table 1). These points define the initial positions of the regression lines for Band 3 and Band 4. The no-change region statistics, such as means, variances, and covariance, are given in Table 2. The ASCR results are given in Table 3. The initially determined locations of the axes of no change obtained by scattergram searching are close to the axes determined by controlled regression refinement for the infrared bands. A total of 6,154,810 pixels fell in the no-change region and were selected by regression. These pixels account for 77.64 percent of the pixels in the whole scene. Thus, the majority of the pixels in the scene contributed to the regression and shared the error of normalization. The RMSs for the no-change region are given in Table 3.

The haze effect in the original image has been significantly reduced in the normalized 1973 image (Plate 1c) and, by visual comparison, one can conclude that the normalized

1973 image provides a better spectral match to the 1990 image than does the raw 1973 image.

Discussion

We have developed an Automatic Scattergram-Controlled Regression (ASCR) for performing relative radiometric normalizations of multispectral images. The ASCR algorithm involves the identification of a set of "no-change" pixels, which are selected using scattergrams of the reference versus the subject images in the near infrared bands. This algorithm has been developed to improve the analysis of land-cover change using recent and historic Landsat MSS data. The ASCR procedure could be used with other types of similar multispectral datasets, such as SPOT or Landsat Thematic Mapper data, as long as the scenes are coregistered.

Compared with other linear radiometric relative rectification methods, the ASCR method has the following advantages: (1) cloud/shadow/snow effects are reduced compared with simple regression method; (2) a large percentage of the total number of image pixels is used; (3) normalization errors are distributed among different land-cover types, preventing error accumulation on some particular land-cover types that might have been introduced by training set selection; (4) the necessity of identifying bright and dark radiometric control pixels is eliminated; and (5) the speed of the normalization procedure is accelerated by reducing human intervention compared with other empirical methods, though it may not necessarily reduce the time of computation.

The ASCR procedure is designed to be applied to imagery acquired under similar solar illumination geometries and similar phenological conditions. The basic assumption of the ASCR method is that land cover for a large portion of the land surface covered has not changed between the subject and reference images. In addition, the procedure requires the presence of both land and water pixels in the scene. Considering the large area covered by Landsat scenes (185 by 185 km), these conditions will generally be met.

Our results indicate that the ASCR method is effective in normalizing the radiometric characteristics of subject images to match reference image, with a minimal amount of human intervention. This procedure should be especially useful for the analysis of land-cover change. Our research is now focusing on the development of an automated procedure for selecting the thresholds used to define the "no-change" pixels.

Acknowledgment

This research was conducted with assistance from the U.S. Environmental Protection Agency, Environmental Monitoring Systems Laboratory, in Las Vegas, Nevada, through Cooperative Agreement #CR816826-02. Although the research described in this article has been supported by the U.S. EPA, it has not been subjected to Agency review and therefore does not necessarily reflect the views of the Agency and no official endorsement should be inferred. Mention of trade names or commercial products does not constitute endorsement or recommendation for use.

References

Hall, F.G., D.E. Strebel, J.E. Nickeson, and S.J. Goetz, 1991. Radiometric rectification: Toward a common radiometric response among multidate, multisensor images, *Remote Sensing of Environment*, 35:11–27.

Jenson, J.R., (editor), 1983. Urban/suburban land use analysis, *Manual of Remote Sensing*, Vol. 2, Second Edition, American Society of Photogrammetry, pp. 1571–1666.

Kauth, R.J., and G.S. Thomas, 1976. The Tasseled Cap—A graphic description of the spectral-temporal development of agricultural crops as seen by Landsat, *Proceedings of the Symposium on Machine Processing of Remotely Sensed Data*, LARS, Purdue University, West Lafayette, Indiana, pp. 41–51.

Lunetta, R.S., J.G. Lyon, J.A. Sturdevant, J.L. Dwyer, C.D. Elvidge, L.K. Fenstermaker, D. Yuan, S.R. Hoffer, and R. Weerackoon, 1993. *North American Landscape Characterization (NALC) Research Plan*, USPA/600/R-93/135, 419 p.

Markham, B.L., and J.L. Barker, 1987. Radiometric properties of U.S. processed Landsat MSS data, *Remote Sensing of Environment*, 22:39–71.

Schott, J.R., C. Salvaggio, and W.J. Volchok, 1988. Radiometric scene normalization using pseudoinvariant features, *Remote Sensing of Environment*, 26:1–16.

Yuan, D., and C.D. Elvidge, 1993. Application of relative radiometric rectification procedure to Landsat data for use in change detection, *Proceedings of the Workshop on Atmospheric Correction of Landsat Imagery*, The Defense Landsat Program Office, Torrance, California, 29 June - 1 July, pp. 162–166.

(Received 7 March 1994; accepted 4 August 1994)

Christopher D. Elvidge
Christopher D. Elvidge received a Ph.D. in Applied Earth Sciences from Stanford University in 1985. He is currently on assignment at the NOAA National Geophysical Data Center in Boulder, Colorado, where he is leading a global inventory of biomass burning.

Ding Yuan
Ding Yuan graduated from the China University of Geoscience with a B.S. in Mathematics (1982) and an M.S. in Geology (1985). In addition, he holds an M.S. in Mathematics (1989) and a Ph.D. in Geology (1991) from Syracuse University. He is an Assistant Research Professor at the Desert Research Institute, where he conducts research on the detection of land-cover change using Landsat data.

Ridgeway Weerackoon
Ridgeway Weerackoon graduated with a B.Sc. in Mathematics from the University Ceylon in 1956. He taught mathematics at the University of Nevada, Las Vegas in 1977. From 1978 to 1992 he worked as a computer programmer for Lockheed in Las Vegas. He is currently a computer programmer for the Desert Research Institute.

Ross S. Lunetta
Ross S. Lunetta holds B.S. and M.S. degrees in biology. He is currently on assignment at the EPA Region X Office in Seattle as an Office of Research and Development Science Advisor. Prior to this assignment, he was the Remote Sensing Program Manager at EPA's Environmental Monitoring Systems Laboratory in Las Vegas, Nevada. From 1991 to 1994 he was Technical Director of EPA's North American Landscape Characterization.